

Isomorphs in flexible Lennard-Jones chains

Arno A. Veldhorst, Jeppe C. Dyre, and Thomas B. Schröder
*DNRF Center “Glass and Time”, IMFUFA, Dept. of Sciences,
 Roskilde University, P.O. Box 260, DK-4000 Roskilde, Denmark*
 (Dated: July 21, 2019)

This paper shows that the model of short, flexible Lennard-Jones chains (LJC) has curves (isomorphs) in its phase diagram along which structure and dynamics are invariant in the appropriate units. The isomorphs are identified by a density-dependent scaling exponent which can be obtained from fluctuations in the configurational parts of the energy and pressure. The isomorph invariance of the dynamics is seen both in segmental and center of mass dynamics, as well as in the relaxation of the Rouse modes. Jumps between different state points on the same isomorph happen instantaneously without any slow relaxation. Our findings show that the isomorph theory not only applies to atomic and small molecular liquids as previously shown, but also to flexible, anisotropic molecules. Since the LJC is a simple model system for alkanes and polymers, our results provide a possible explanation for why power-law density scaling is observed experimentally in alkanes and many polymeric systems. The theory provides an independent mean of determining the scaling exponent, which is usually treated as an empirical scaling parameter.

INTRODUCTION

The dynamics of glass-forming liquids slows down dramatically upon cooling or compression. The dynamics in general depends on two variables, density and temperature (or pressure and temperature). However, it was observed experimentally that the dynamics, e.g., quantified via the dielectric relaxation time, of a large group of glass formers including polymers can be scaled onto a single curve [1–4], showing that the relaxation time is a function of $h(\rho)/T$, where ρ is the density. There was some debate over the functional form of $h(\rho)$ and whether it could be uniquely determined given the limited density changes experimentally available [5–10]. In a famous review Roland et al. [11] demonstrated that scaling with $h(\rho) = \rho^\gamma$ with a material specific scaling exponent γ works well for a large group of organic glass formers, including polymers. We refer to this scaling as power-law density scaling.

Power-law density scaling is exact for atomic systems with inverse power-law (IPL) pair potentials, $v(r) = \varepsilon(r/\sigma)^{-n}$, in which γ is related to the exponent of the potential via $\gamma = n/3$. It turns out, however, that many different molecular systems obey power-law density scaling, including the aforementioned polymers, but also ionic liquids [12–16] and liquid crystals [17–22].

The isomorph theory was published in 2009 [23, 24]. It predicts for a class of liquids the existence of “isomorphs”, which are curves in the phase diagram along which structure and dynamics are invariant in the appropriate “reduced” units. Also the excess entropy and the isochoric specific heat are predicted to be invariant on isomorphs. Since both excess entropy and the relaxation times are predicted to be constant on an isomorph, the isomorph theory is consistent with Rosenfeld’s excess entropy scaling [23, 25, 26], according to which liquids’ transport coefficients are a function of ex-

cess entropy only.

Many different systems have been shown to have approximate isomorphs in their phase diagram; simple atomic model systems [23, 27], as well as small, rigid molecular models have been studied [28]. The isomorph theory predicts “isomorph scaling”, i.e., that the dynamics is a function of $h(\rho)/T$, where $h(\rho)$ depends on the system [29, 30]. For atomic systems interacting via the Lennard-Jones potential $h(\rho)$ is known analytically, $h(\rho) = (\gamma_0/2 - 1)\rho^4(\gamma_0/2 - 2)\rho^2$ where γ_0 is γ at density unity. For many other systems however, $h(\rho)$ is not known analytically. Power-law density scaling is an approximation to isomorph scaling which can be used if the density changes are not too large. In this case the theory provides an independent way of determining the scaling exponent (where U is the potential energy, W is the virial, Δ denotes deviation from thermal average, and brackets $\langle \dots \rangle$ denote average in the canonical ensemble):

$$\gamma = \frac{\langle \Delta W \Delta U \rangle}{\langle (\Delta U)^2 \rangle}. \quad (1)$$

Liquids that have isomorphs in their phase diagram also have strong correlations between the constant-volume fluctuations of the the potential energy U and the virial W [31, 32], where the virial W is the configurational contribution to the pressure: $pV = Nk_B T + W$. The U, W correlations are quantified via the correlation coefficient,

$$R = \frac{\langle \Delta W \Delta U \rangle}{\sqrt{\langle (\Delta W)^2 \rangle \langle (\Delta U)^2 \rangle}}. \quad (2)$$

Once again the IPL liquids have perfect correlations, $R = 1$, but a large group of liquids have a correlation coefficient close to one, indicating strong correlation. Liquids with a correlation larger than 0.9 were referred to as “strongly correlating”, but since this term was often confused with strongly correlated quantum systems, we

now refer to this group of liquids as Roskilde-simple liquids. It is a prediction of the isomorph theory that this group of simple liquids obeys isomorphic scaling [23, 33].

The isomorph theory has so far only been tested for atomic liquids and rigid molecules, while most organic glass formers are much larger, often flexible molecules. Since both alkanes [14, 34, 35] and polymers [11, 36] have been shown to obey power-law density scaling, we have chosen to apply the isomorph theory to a liquid of linear, flexible molecules.

SIMULATION DETAILS

We performed Molecular Dynamics simulations of flexible Lennard-Jones chains (LJCs) consisting of 10 bonded segments. Segments in different molecules and non-bonded segments within a molecule interact via the standard LJ potential, cutting and shifting the potential at 2.5σ . We simulated 200 chains in a cubic bounding box with periodic boundary conditions, in the NVT ensemble using a Nosé-Hoover thermostat. For the time step we used $\Delta t = 0.0025$, and the time constant of the thermostat was 0.2. The simulation was performed with our RUMD [37] software utilizing state of the art GPU computing.

The model has been derived from a model by Kremer and Grest [38], who did not include the attractive part of the LJ potential. The model including the LJ attraction has been used extensively for viscous polymer melts close to the glass transition [39–43]. With our purpose in mind, the model is of special interest since it has already been shown to obey both Rosenfeld’s excess entropy scaling [35, 44, 45] and power-law density scaling [35] to some degree.

Short LJ chains of around ten segments have been used extensively to simulate glassy polymer melts [46–49], even though real polymers easily consist of thousands of monomers. The reason for this is threefold. Firstly, the LJC is a coarse-grained model, meaning that a single Lennard-Jones particle may correspond to several monomers. Secondly, increasing the chain length in general increases the total system size, which in turn increases the simulation time. Most importantly, it is often the equilibrium (viscous) liquid that is of interest. Both increasing the chain length and approaching the glass transition increase the equilibration time, meaning that there is always a trade-off between chain length and viscosity [50, 51].

Usually, the neighboring segments in the chain are bonded by a FENE potential, although harmonic springs [41–43] and rigid bonds [35, 44, 45] have also been used. Here, the bond length $l_b = \sigma = 1$ was kept constant using the Time Symmetrical Central Difference algorithm [52, 53]. Like other constraint algorithms, these bonds contribute to the virial [54]: $W_{total} =$

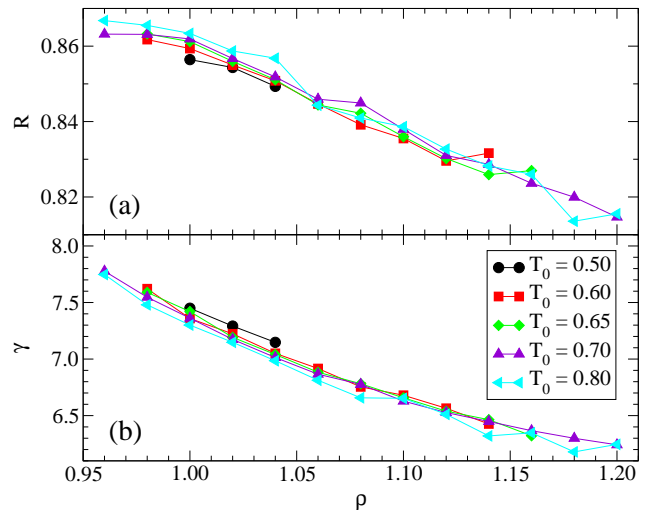


FIG. 1. (a) The correlation coefficient R , calculated from the instantaneous values of the virial W and the potential energy U using Eq. (2). Each data set corresponds to an isomorph, obtained as described in the text. The correlation coefficient is high, albeit lower than for a standard single component Lennard-Jones liquid [55]. (b) The isomorphic scaling exponent γ as defined by Eq. (1). The values found are significantly higher than for the single component Lennard-Jones liquids [55], and show a clear density dependence. The logarithmic derivatives of γ on the isochore and isotherm confirm that γ is much more dependent on the density: $(\frac{\partial \ln \gamma}{\partial \ln T})_{\rho=1} \approx 0.05$ and $(\frac{\partial \ln \gamma}{\partial \ln \rho})_{T=0.7} \approx 0.89$, as predicted by the isomorph theory.

$$W_{LJ} + W_{constraint}.$$

RESULTS AND DISCUSSION

To generate an isomorph, a NVT simulation was performed at a state point (ρ_0, T_0) , and the scaling exponent γ was calculated using Eq. (1). Since the excess (configurational) entropy $S_{ex} = S - S_{ideal}$ is predicted to be constant on an isomorph, the following identity can then be used to get the new temperature after a small (0.02) change in density [23]:

$$\gamma = \left(\frac{\partial \ln T}{\partial \ln \rho} \right)_{S_{ex}}. \quad (3)$$

Applying this procedure iteratively will generate a curve with constant S_{ex} . If the model conforms to the isomorph theory, this curve will be an isomorph, i.e., have invariant dynamics and structure in reduced units. Five isomorphs were generated using this procedure with $\rho_0 = 1.0$ and $T_0 = \{0.5, 0.6, 0.65, 0.7, 0.8\}$.

In Fig. 1(a), the correlation coefficient R is plotted as a function of density for the five isomorphs. For the densities we have simulated, the correlation coefficient varies between 0.81 and 0.87, which is lower than the (somewhat arbitrary) 0.9 limit for simple liquids. However, we

show with this paper, that the LJC model also shows clear isomorphs in its phase diagram, and that within the density range investigated, simple power-law density scaling does not suffice.

In Fig. 1(b) we plot the values of γ calculated from Eq. (1). The isomorph theory predicts γ to depend on density but not temperature [23, 24]. This is seen to be fulfilled to a good approximation; γ is seen to change much more by increasing density by 25% than by increasing temperature by 60%. The density dependence of γ means that we can only use Eq. (3) for small density changes, and indicates that simple power-law density scaling is an approximation that only works for small density changes.

The γ values found for the LJC model (6.1–7.9) are higher than for a single component LJ liquid (5.3–6.7) [32]. This increase in γ is due to the fixed constraints, which can be seen as a very steep repulsion between bonded segments. On the other hand, the high γ values is in contrast to the values found from power-law density scaling, which are generally lower for polymers than for small molecular liquids [36]. Tsolou et al [56] found $\gamma = 2.8$ from power-law density scaling of simulation data of a united atom model of *cis*-1,4-polybutadiene. A possible explanation for this low value of γ has been given by Xu [57] who showed using the generalized entropy theory that polymer rigidity significantly decreases the density scaling exponent γ .

In the following, we test a number of isomorph predictions focusing on the $(\rho_0, T_0) = (1.0, 0.7)$ isomorph, before returning to the question of the overall scaling properties of the model. The isomorph theory predicts dynamics and structure to be invariant on an isomorph. This invariance applies to data in reduced units, which means that distance and time are scaled using $\tilde{r} = \rho^{1/3}r$ and $\tilde{t} = \rho^{1/3}(T/m)^{1/2}t$, where m is the mass of a segment [23, 58]. The dynamics are of particular interest here, because the dependence on state point becomes large upon cooling and/or compression. In Fig. 2(a), different dynamical quantities are plotted. The self part of the segmental and the center of mass intermediate scattering function $F_S(q, t)$, as well as the orientational autocorrelation of the end-to-end vector $\langle \mathbf{R}(0)\mathbf{R}(t) \rangle$ are plotted as a function of reduced time. The values of q were kept constant in reduced units: $q = \tilde{q}\rho^{1/3}$. All these measures of the dynamics collapse well for the isomorph state points compared to an isothermal density change; Increasing the density by 11% while keeping temperature constant significantly changes the dynamics, whereas increasing the density 25% while following the isomorph keeps the dynamics invariant to a really good approximation.

We define a relaxation time for the dynamical quantities as the time where the correlation function reaches 0.2. These relaxation times are plotted in Fig. 3, this time also varying q . The different relaxation times char-

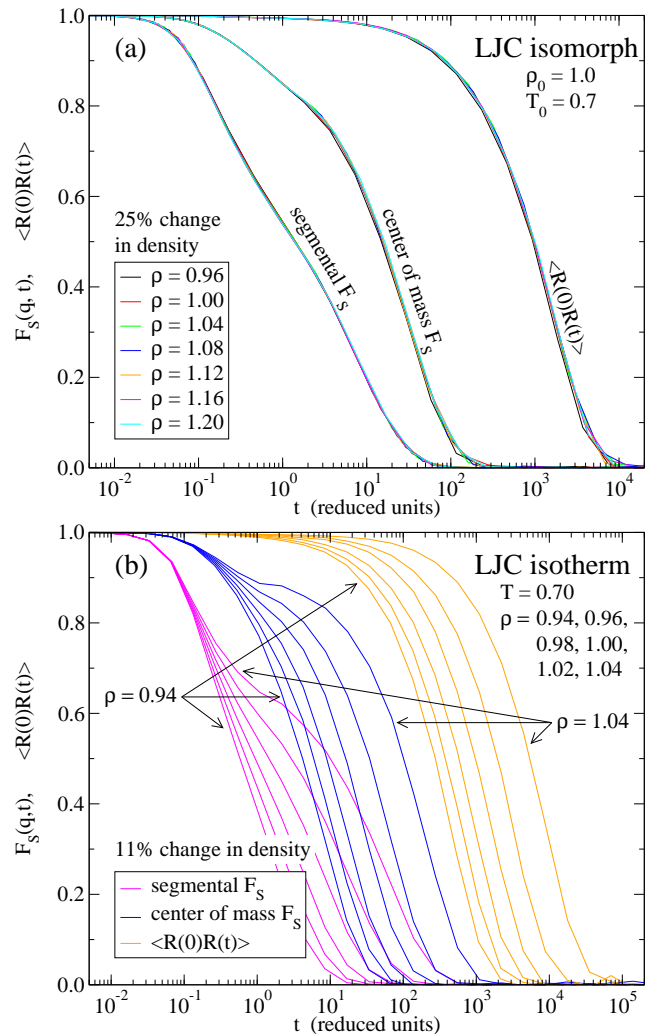


FIG. 2. The segmental and center of mass intermediate scattering function $F_S(q, t)$, as well as the orientational correlation function of the end-to-end vector $\langle \mathbf{R}(t)\mathbf{R}(0) \rangle$. The position of the peak of the (segmental) static structure factor was taken as the value for q . (a) The data for 7 isomorph state points collapse on a single master curve when plotted in reduced units, and this is the case for all three relaxation functions. (b) For isothermal state points, the curves do not collapse but are spread over a larger dynamical range.

acterizing the dynamics covers more than 4 decades in time, but each of them are to a good approximation invariant on the isomorph. In contrast, the relaxation times on the isotherm shown (open red symbols) shows a clear dependence on density.

The dynamics of flexible chains are often expressed in terms of correlation functions of Rouse modes, $\langle \mathbf{X}_p(t)\mathbf{X}_q(0) \rangle$ [59, 60]. The zeroth mode describes the center of mass displacement of the chain, while the other modes describe vibrations in a subchain of N/p segments. In Fig. 4 some of the Rouse mode auto correlation functions are plotted for the isomorph state points. For the lower modes, there is an excellent collapse of the corre-

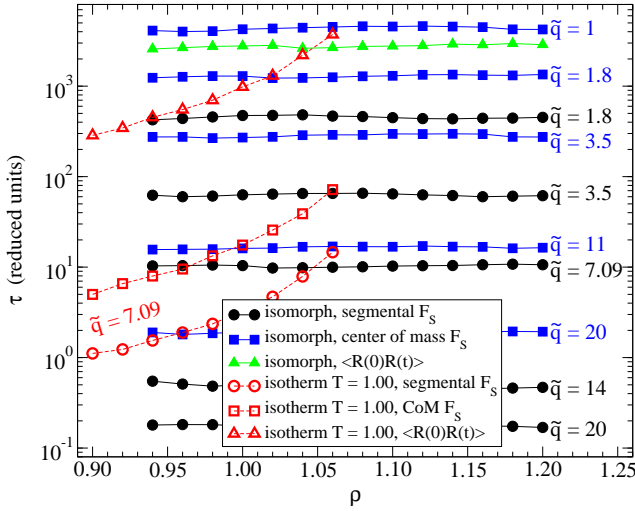


FIG. 3. Relaxation times calculated from the orientational autocorrelation of the end-to-end vector and the intermediate scattering function, as function of density. The value of the \tilde{q} vector has been varied to obtain different measures of the relaxation time. Each value was kept constant in reduced units for the different densities. All relaxation time measures are invariant for isomorph state points (filled symbols). An isotherm is included for comparison (open red symbols).

lation functions, whereas the invariance decreases somewhat for the higher modes. It should however be noted that the amplitude of the rouse modes is predicted to scale as $\langle X_p^2 \rangle \propto 1/(N \sin^2(p/N))$, so the contribution of the higher modes is very small [61].

Fig. 5 shows the isomorph invariance of the mean square displacement of both the segments and the center of mass in all regimes, including the subdiffusive regimes which is specific for polymers and other flexible molecules.

Not only equilibrium dynamics, but also out of equilibrium dynamics are predicted to be invariant on an isomorph. We test this by changing density and temperature instantaneously during the simulation. The center of mass positions are scaled together with the box, but the intramolecular distances were kept constant. In Fig. 6 the relaxation of the potential energy is plotted after different instantaneous jumps. The figure shows that no relaxation is visible in the energy when jumping between two state points that are isomorph to each other (black line). This is predicted by the isomorph theory: two state points on the same isomorph are equivalent with regard for aging [23]. Likewise, when jumping from two state points on the same isomorph to a third state point that is not on that isomorph, the relaxation curve is the same for the two jumps. When the density is changed, the system is immediately in equilibrium at the isomorph state point with the new density. Any relaxation after the density jump then takes place on the isochore [62].

Also the structure is predicted to be invariant on an

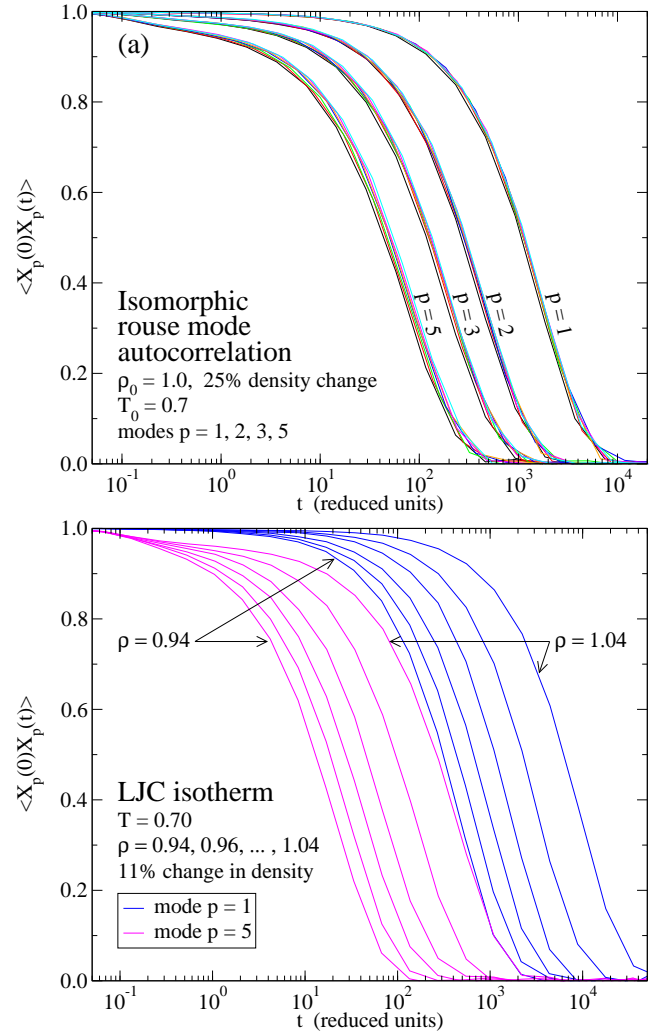


FIG. 4. Auto-correlation functions of some rouse modes. (a) For the same isomorph state points as in Fig. 2(a). The collapse of the Rouse modes is good, especially for the lower modes. (b) Data for the same isothermal state points as in Fig. 2(b). There is no collapse of the dynamics for isothermal state points.

isomorph [23]. However, not all structural quantities are necessarily equally invariant when molecular liquids are considered. Consider for instance a rigid, covalent bond. Since the bond length is constant in normal units and does not change with density, the bond length in reduced units will not be constant on the isomorph in reduced units. For that reason we plot the inter- and intramolecular contribution to the segmental radial distribution function $g(r)$ separately in Fig. 7. The intermolecular structure is quite constant on the isomorph, while the intramolecular structure is clearly not. The center of mass $g(\tilde{r})$ was also found to be invariant on the isomorph when plotted in reduced units (data not shown), but it is also invariant on the isochore and isotherm within the liquid (fluid) phase.

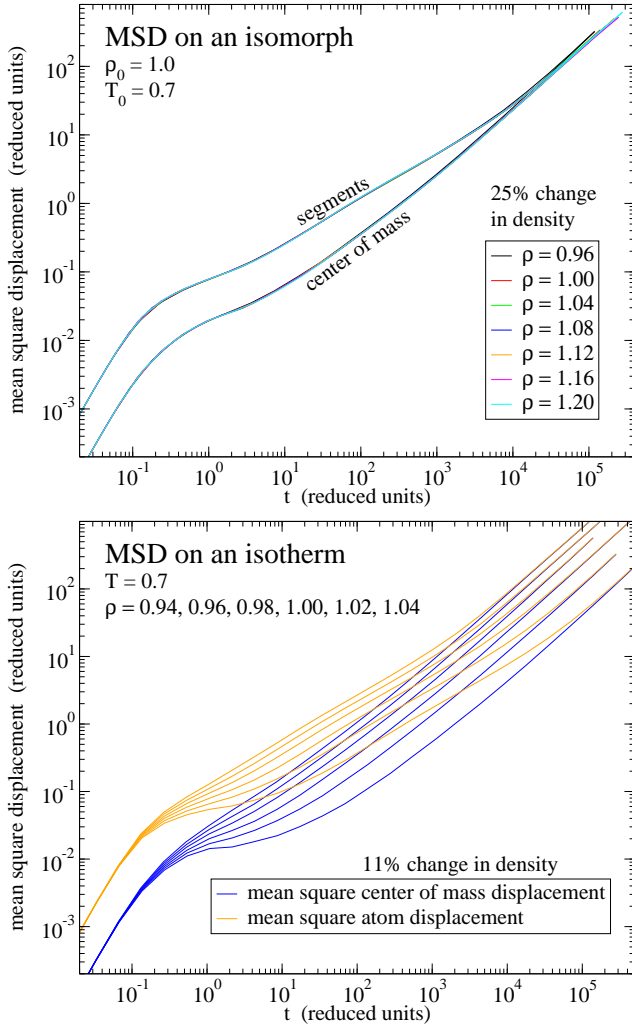


FIG. 5. The mean square displacements of the segments and the center of mass of the chains. (a) again, there is a good collapse for the mean square displacement on the isomorph, for both the segments and the center of mass. (b) This is not the case for the isotherm.

To investigate the difference in inter- and intramolecular structure further, we plot the mean square radius of gyration $\langle R_g^2 \rangle$ and the mean square end-to-end vector $\langle R^2 \rangle$ in Fig. 8. These intramolecular quantities are clearly not invariant on the isomorph, changing as much with density as on the isotherm. On an isochore these quantities are even more constant than on the isomorph. The lack of temperature dependence of these quantities was already noted for a similar bead-spring model [63].

Finally, we return to the question of the overall scaling of the dynamics of the model. As mentioned in the introduction, the isomorph theory predicts that each relaxation time characterizing the dynamics is a function of $h(\rho)/T$ where $h(\rho)$ is system dependent function. For atomic system with pair potentials being sums of power laws, we have an analytical expression for $h(\rho)$ [29]. Due

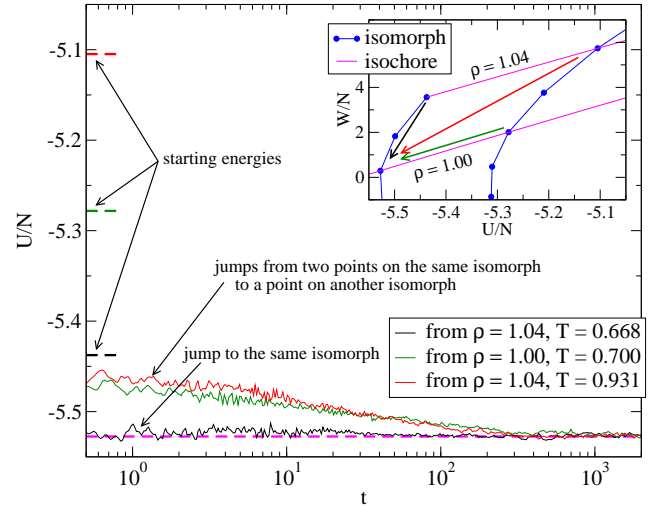


FIG. 6. Potential energy relaxation after instantaneous jumps from three different state points to $\rho = 1.00, T = 0.50$. The inset shows the direction of the jumps in the phase diagram, plotted in the U, W -plane. Black line: a jump between isomorph state points. The energy shows no relaxation since the system is immediately in equilibrium. Red and green lines: two jumps from the same isomorph to another isomorph show the same relaxation behavior. The data of the relaxation plots are averaged of 8 independent starting configurations.

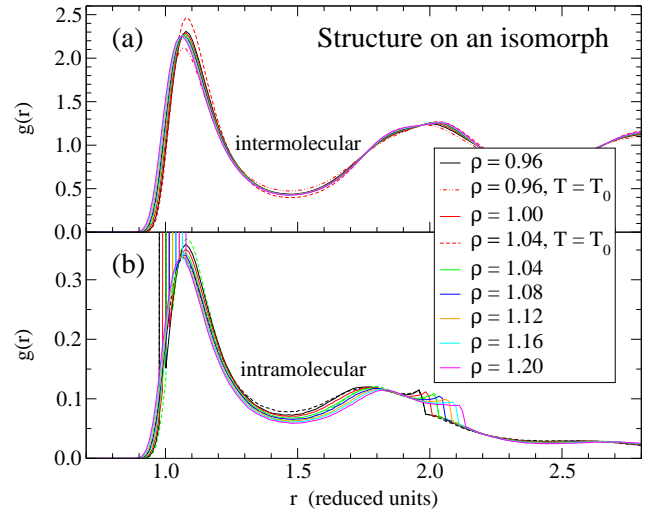


FIG. 7. Segmental and molecular structure on an isomorph for the same state points as in Fig. 2. Dashed lines correspond to isothermal density changes and are included for comparison. The data show that intermolecular structure is invariant, while intramolecular structure is not invariant on the isomorph due to the constant bond length. (a) The intermolecular (segmental) radial distribution function $g(\tilde{r})$ in reduced units on the isomorph $(\rho, T) = (1.00, 0.70)$. The intermolecular $g(r)$ is to a good degree invariant for isomorph state points, especially when compared to a (small) density change on an isotherm. (b) The intramolecular $g(r)$ is clearly not invariant on an isomorph.

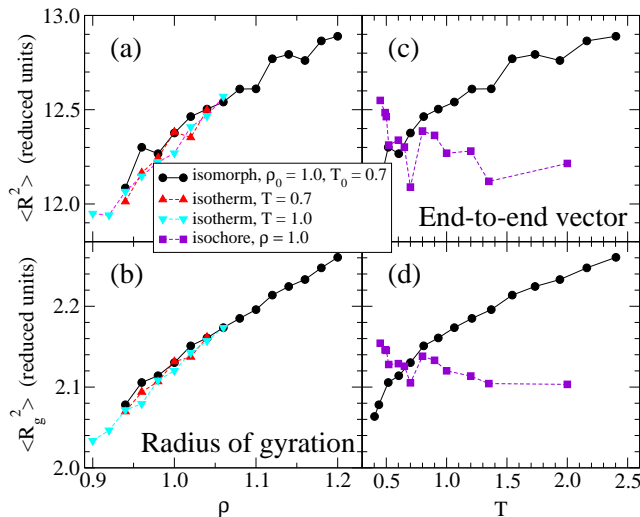


FIG. 8. Intramolecular quantities are not invariant on the isomorph (black solid lines) (a) The mean square end-to-end vector $\langle R^2 \rangle$ and the mean square radius of gyration (b) as a function of density. The temperature dependence of these quantities is similar on the isomorph and isotherms (dashed lines). It should be mentioned that when these quantities are plotted in real units, they show an (intuitive) decrease with density. (c) and (d) The same data for the isomorph state points, now plotted as a function of temperature and compared with an isochore. These intramolecular quantities are actually more constant on the isochore, due to the fixed bond length.

to the presence of the bonds, we unfortunately do *not* have an analytical expression for $h(\rho)$ in the model studied here. Fig. 9 shows the five studied isomorph in the ρ, T plane (filled symbols). The open symbols show the same data, except that the temperatures are divided by T_0 (the temperature at $\rho = 1$). The scaled data is predicted to collapse on a single curve, $h(\rho)$, which is indeed seen to be the case. We find $h(\rho)$ to be well approximated by $h(\rho) = 2\rho^{5.06} - \rho^{2.61}$, where the two exponents were determined by fitting.

Fig. 10 compares for three isochores the power-law density scaling and the scaling predicted by the isomorph theory. Fig. 10(a) and Fig. 10(b) show that the two smallest densities collapse using power-law density scaling with $\gamma = 7.7$, whereas the two highest densities collapse using $\gamma = 6.7$. Notice that the values of γ found by this empirical scaling is consistent with the values found from the W, U fluctuations in the respective density intervals (see Fig. 1). The power-law density scaling is thus an approximation that works for (relatively) small density changes, and the scaling exponent γ can be determined independently from the W, U -fluctuations. The more general form of scaling is the one predicted by the isomorph theory, which is tested in Fig. 10(c), using the $h(\rho)$ determined empirically in Fig. 9. The collapse is seen to be excellent. Notice that the isomorph scaling

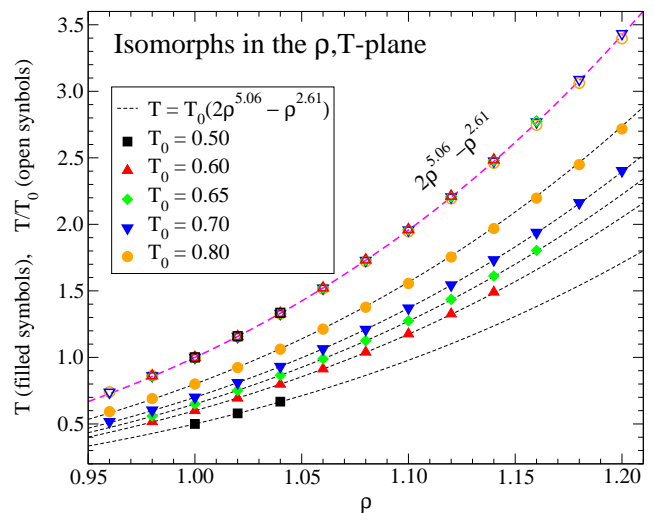


FIG. 9. Filled symbols: Shape of isomorphs in the ρ, T -plane. Open symbols: Same data with temperatures divided by T_0 , showing a good collapse as predicted by the isomorph theory. Dashed lines: The function $h(\rho)$ was found by fitting to the open symbols (see text).

also captures the different shapes of the segmental and chain dynamics, which is also well known for power-law density scaling in a small density range [64–66]. Moreover, it has recently been suggested that for a wider group of glass formers both the α -relaxation and the Johari-Goldstein β -relaxation obey power-law density scaling with the same value of γ , even though these relaxation times have a completely different dependence on density or ρ^γ/T [67]. However, the validity this result, especially in the liquid phase, is still under discussion [68].

CONCLUSION

To summarize, we have shown that the predictions of the isomorph theory apply to a flexible chain-like model system, despite the fact that the system is not entirely “Roskilde-simple” because $R < 0.9$. The isomorph invariance of structural quantities is not quite as good as for previously studied atomic systems, and also the pressure - energy correlations are not as strong. However, the collapse of the dynamics at different time scales is unmistakable, and works for the segmental dynamics as well as the chain dynamics. This indicates that the isomorph theory may be extended to include flexible molecules. In particular this explains the experimentally observed power-law density scaling for alkanes and many polymers - and predicts that it should break down at larger density variations where isomorph scaling is needed.

The centre for viscous liquid dynamics “Glass and Time” is sponsored by the Danish National Research Foundation via Grant No. DNRF61.

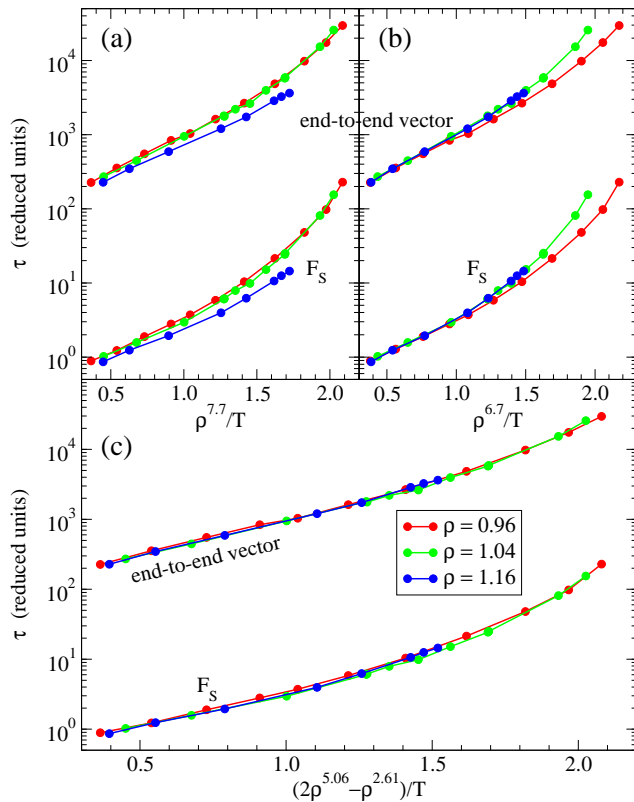


FIG. 10. Comparison between power-law density scaling and isomorph density scaling, applied to the relaxation times of the end-to-end vector and the segmental incoherent intermediate scattering function (F_S). (a) and (b) The power-law density scaling approach for two different values of γ (7.7 and 6.7), collapsing the low and high density isochores respectively. Neither value gives a good collapse of all the data. (c) Isomorph scaling approach, using the function $h(\rho) = 2\rho^{5.06} - \rho^{2.61}$ (see Fig. 9) to scale the relaxation times, giving a much better collapse. It should be noted that for the lowest density some of the slowest state points have a negative pressure. Although this is of unphysical, it should be noted that the liquid is still homogeneous due to the finite but constant size of the simulation box.

[1] A. Tölle, Reports on Progress in Physics **64**, 1473 (2001)
[2] C. Alba-Simionesco, D. Kivelson, and G. Tarjus, J. Chem. Phys. **116**, 5033 (2002)
[3] C. Dreyfus, A. Aouadi, J. Gapinski, M. Matos-Lopes, W. Steffen, A. Patkowski, and R. M. Pick, Phys. Rev. E **68**, 011204 (2003)
[4] M. Paluch, R. Casalini, A. Patkowski, T. Pakula, and C. M. Roland, Phys. Rev. E **68**, 031802 (2003)
[5] G. Tarjus, D. Kivelson, S. Mossa, and C. Alba-Simionesco, J. Chem. Phys. **120**, 6135 (2004)
[6] R. Casalini and C. M. Roland, Phys. Rev. E **69**, 062501 (2004)
[7] C. M. Roland and R. Casalini, J. Chem. Phys. **121**, 11503 (2004)

[8] G. Tarjus, S. Mossa, and C. Alba-Simionesco, J. Chem. Phys. **121**, 11505 (2004)
[9] C. Alba-Simionesco, A. Cailliaux, A. Alegría, and G. Tarjus, Europhys. Lett. **68**, 58 (2004)
[10] C. Dreyfus, A. Le Grand, J. Gapinski, W. Steffen, and A. Patkowski, Eur. Phys. J. B **42**, 309 (2004)
[11] C. M. Roland, S. Hensel-Bielowka, M. Paluch, and R. Casalini, Reports on Progress in Physics **68**, 1405 (2005)
[12] M. Paluch, S. Haracz, A. Grzybowski, M. Mierzwa, J. Pionteck, A. Rivera-Calzada, and C. Leon, J. Phys. Chem. Lett. **1**, 987 (2010)
[13] J. Habasaki, R. Casalini, and K. L. Ngai, J. Phys. Chem. B **114**, 3902 (2010)
[14] E. R. López, A. S. Pensado, M. J. P. Comuñas, A. A. H. Pádua, J. Fernández, and K. R. Harris, J. Chem. Phys. **134**, 144507 (2011)
[15] A. Swiety-Pospiech, Z. Wojnarowska, J. Pionteck, S. Pawlus, A. Grzybowski, S. Hensel-Bielowka, K. Grzybowski, A. Szulc, and M. Paluch, J. Chem. Phys. **136**, 224501 (2012)
[16] A. Swiety-Pospiech, Z. Wojnarowska, S. Hensel-Bielowka, J. Pionteck, and M. Paluch, J. Chem. Phys. **138**, 204502 (2013)
[17] S. Urban and A. Würflinger, Phys. Rev. E **72**, 021707 (2005)
[18] S. Urban, C. M. Roland, J. Czub, and K. Skrzypek, J. Chem. Phys. **127**, 094901 (2007)
[19] C. M. Roland, R. B. Bogoslovov, R. Casalini, A. R. Ellis, S. Bair, S. J. Rzoska, K. Czuprynski, and S. Urban, J. Chem. Phys. **128**, 224506 (2008)
[20] S. Urban and C. M. Roland, J. Non-Cryst Solids **357**, 740 (2011)
[21] S. Urban, Liq. Cryst. **38**, 1147 (2011)
[22] K. Satoh, J. Chem. Phys. **138**, 094903 (2013)
[23] N. Gnan, T. B. Schröder, U. R. Pedersen, N. P. Bailey, and J. C. Dyre, J. Chem. Phys. **131**, 234504 (2009)
[24] T. B. Schröder, N. Gnan, U. R. Pedersen, N. P. Bailey, and J. C. Dyre, J. Chem. Phys. **134**, 164505 (2011)
[25] Y. Rosenfeld, Phys. Rev. A **15**, 2545 (1977)
[26] M. Dzugutov, Nature **381**, 137 (1996)
[27] A. A. Veldhorst, L. Böhling, J. C. Dyre, and T. B. Schröder, Eur. Phys. J. B **85**, 21 (2012)
[28] T. S. Ingebrigtsen, T. B. Schröder, and J. C. Dyre, J. Phys. Chem. B **116**, 1018 (2012)
[29] T. S. Ingebrigtsen, L. Böhling, T. B. Schröder, and J. C. Dyre, J. Chem. Phys. **136**, 061102 (2012)
[30] L. Böhling, T. S. Ingebrigtsen, A. Grzybowski, M. Paluch, J. C. Dyre, and T. B. Schröder, New Journal of Physics **14**, 113035 (2012)
[31] U. R. Pedersen, N. P. Bailey, T. B. Schröder, and J. C. Dyre, Phys. Rev. Lett. **100**, 015701 (2008)
[32] N. P. Bailey, U. R. Pedersen, N. Gnan, T. B. Schröder, and J. C. Dyre, J. Chem. Phys. **129**, 184507 (2008)
[33] T. S. Ingebrigtsen, T. B. Schröder, and J. C. Dyre, Phys. Rev. X **2**, 011011 (2012)
[34] A. S. Pensado, A. A. H. Pádua, M. J. P. Comuñas, and J. Fernández, J. Phys. Chem. B **112**, 5563 (2008)
[35] G. Galliero, C. Boned, and J. Fernández, J. Chem. Phys. **134**, 064505 (2011)
[36] C. M. Roland, Macromolecules **43**, 7875 (2010)
[37] "Roskilde University Molecular Dynamics," <http://rumd.org>

- [38] K. Kremer and G. S. Grest, *J. Chem. Phys.* **92**, 5057 (1990)
- [39] C. Bennemann, C. Donati, J. Baschnagel, and S. C. Glotzer, *Nature* **399**, 246 (1999)
- [40] K. Binder, J. Baschnagel, and W. Paul, *Prog. Polym. Sci.* **28**, 115 (2003)
- [41] R. A. Riggleman, G. N. Toepperwein, G. J. Papakonstantopoulos, and J. J. de Pablo, *Macromolecules* **42**, 3632 (2009)
- [42] R. A. Riggleman, J. F. Douglas, and J. J. de Pablo, *Soft Matter* **6**, 292 (2010)
- [43] A. Shavit, J. F. Douglas, and R. A. Riggleman, *J. Chem. Phys.* **138**, 12A528 (2013)
- [44] T. Goel, C. N. Patra, T. Mukherjee, and C. Chakravarty, *J. Chem. Phys.* **129**, 164904 (2008)
- [45] G. Galliero and C. Boned, *Phys. Rev. E* **80**, 061202 (2009)
- [46] C. Bennemann, W. Paul, K. Binder, and B. Dünweg, *Phys. Rev. E* **57**, 843 (1998)
- [47] M. Aichele, Y. Gebremichael, F. W. Starr, J. Baschnagel, and S. C. Glotzer, *J. Chem. Phys.* **119**, 5290 (2003)
- [48] F. Puosi and D. Leporini, *J. Phys. Chem. B* **115**, 14046 (2011)
- [49] F. Puosi and D. Leporini, *J. Chem. Phys.* **136**, 211101 (2012)
- [50] S. C. Glotzer and W. Paul, *Annu. Rev. Mater. Res.* **32**, 401 (2002)
- [51] J.-L. Barrat, J. Baschnagel, and A. Lyulin, *Soft Matter* **6**, 3430 (2010)
- [52] S. Toxvaerd, O. J. Heilmann, T. Ingebrigtsen, T. B. Schröder, and J. C. Dyre, *J. Chem. Phys.* **131**, 064102 (2009)
- [53] T. Ingebrigtsen, O. J. Heilmann, S. Toxvaerd, and J. C. Dyre, *J. Chem. Phys.* **132**, 154106 (2010)
- [54] M. P. Allen and D. J. Tildesley, *Computer simulations of liquids* (Oxford University Press, 1987)
- [55] N. P. Bailey, U. R. Pedersen, N. Gnan, T. B. Schröder, and J. C. Dyre, *J. Chem. Phys.* **129**, 184508 (2008)
- [56] G. Tsolou, V. A. Harmandaris, and V. G. Mavrantzas, *J. Chem. Phys.* **124**, 084906 (2006)
- [57] W.-S. Xu and K. F. Freed, *J. Chem. Phys.* **138**, 234501 (2013)
- [58] D. Fragiadakis and C. M. Roland, *J. Chem. Phys.* **134**, 044504 (2011)
- [59] P. H. Verdier, *J. Chem. Phys.* **45**, 2118 (1966)
- [60] M. Doi and S. F. Edwards, *The theory of polymer dynamics* (Oxford Science Publications, 1986)
- [61] C. Bennemann, J. Baschnagel, W. Paul, and K. Binder, *Computational and theoretical Polymer Science* **9**, 217 (1999)
- [62] N. Gnan, C. Maggi, T. B. Schröder, and J. C. Dyre, *Phys. Rev. Lett.* **104**, 125902 (2010)
- [63] C. Bennemann, J. Baschnagel, and W. Paul, *Eur. Phys. J. B* **19**, 323 (1999)
- [64] C. M. Roland, M. Paluch, and R. Casalini, *Journal of Polymer Science: Part B: Polymer Physics* **42**, 4313 (2004)
- [65] R. Casalini and C. M. Roland, *Macromolecules* **38**, 1779 (2005)
- [66] C. M. Roland, *Curr. Opin. Solid State Mater. Sci.* **11**, 41 (2007)
- [67] K. L. Ngai, J. Habasaki, D. Prevosto, S. Capaccioli, and M. Paluch, *J. Chem. Phys.* **137**, 034511 (2012)
- [68] R. Casalini and C. M. Roland, *Macromolecules* **46**, 6364 (2013)